Supplementary Figure S5

A

```
  1 MFSMRIVCLV LSVVGTAWTA DSGEGDFLAE GGGVRGPRVV ERHQSACKDS
 51 DWPFCSDEDW NYKCPSGCRM KGLIDEVNQD FTNRINKLKN SLFEYQKNNK
101 DSHSLTTNIM EILRGDFSSA NNRDNTYNRV SEDLRSRIEV LKRKVIEKVQ
151 HIQLLQKNVR AQLVDMKRLE VDIDIKIRSC RGSWSRALAR EVDLKDYEDQ
201 QKQLEQVIAK DLLPSRDRQH LPLIKMKPVP DLVPGNFKSQ LQKVPPEWKA
251 LTDMPQMRME LERPGGNEIT RGGSTSYGTG SETESPRNPS SAGSWNSGSS
301 GPGSTGNRNP GSSGTGGTAT WKPGSSGPGS AGSWNSGSSG TGSTGNQNPG
351 SPRPGSTGTW NPGSSERGSA GHWTSESSVS GSTGQWHSES GSFRPDSPGS
401 GNARPNNPDW GTFEEVSGNV SPGTRREYHT EKLVTSKGDK ELRTGKEKVT
451 SGSTTTTRRS CSKTVTKTVI GPDGHKEVTK EVVTSEDGSD CPEAMDLGTL
501 SGIGTLDGFR HRHPDEAAFF DTASTGKTFP GFFSPMLGEF VSETESRGSE
551 SGIFTNTKES SSHHPGIAEF PSRGKSSSYS KQFTSSTSYN RGDSTFESKS
601 YKMADEAGSE ADHEGTHSTK RGHAKSRPVR GIHTSPLGKP SLSP
```

B

4-Hydroxyproline

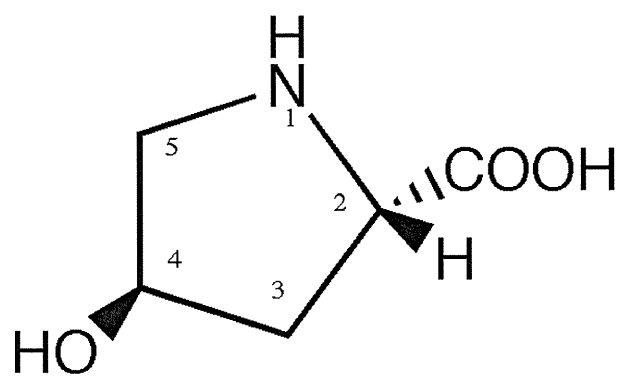

ESSSHHP(O)GIAEFPSR

TFP(O)GFFSPMLGEFVSETESR

Supplementary Figure S6

A

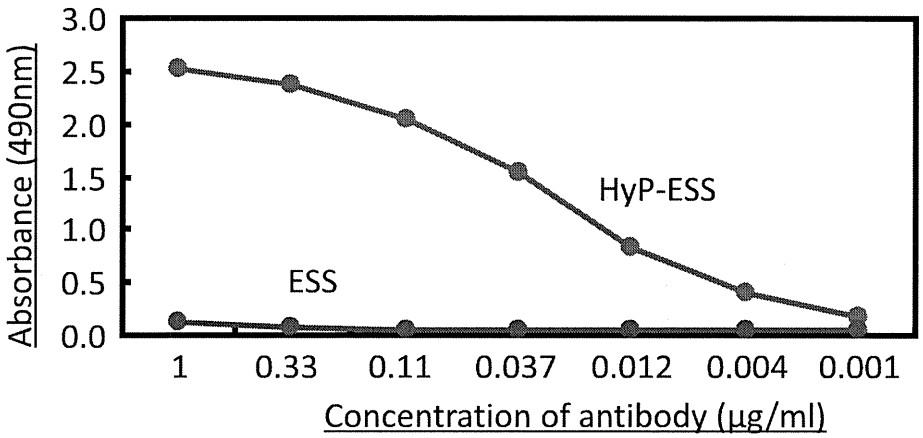

B

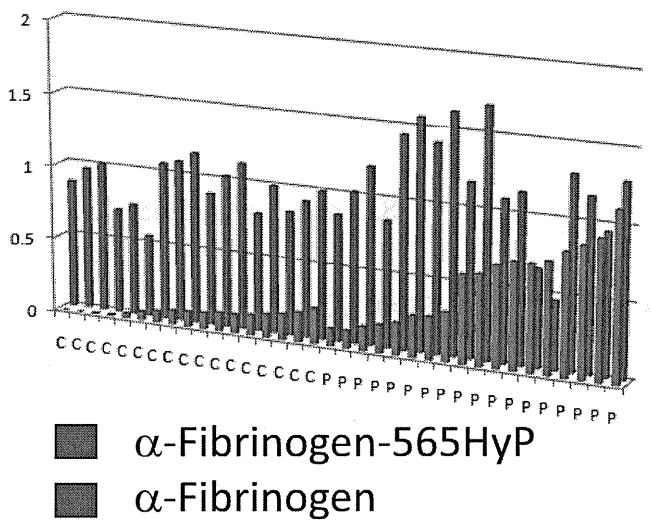

C

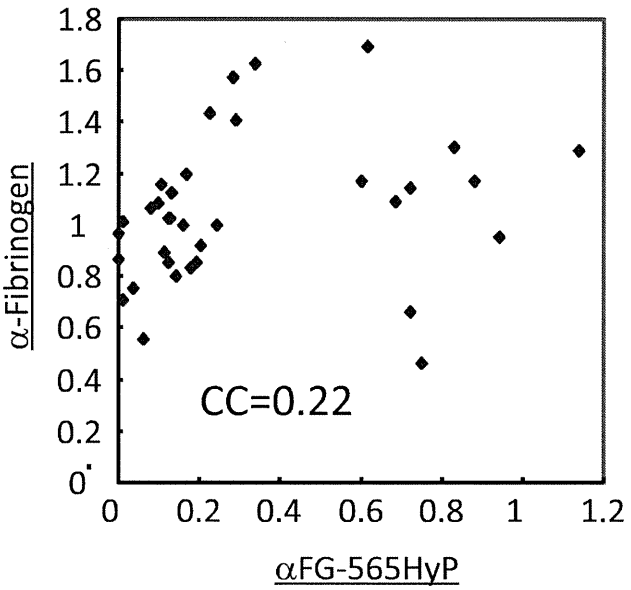

D

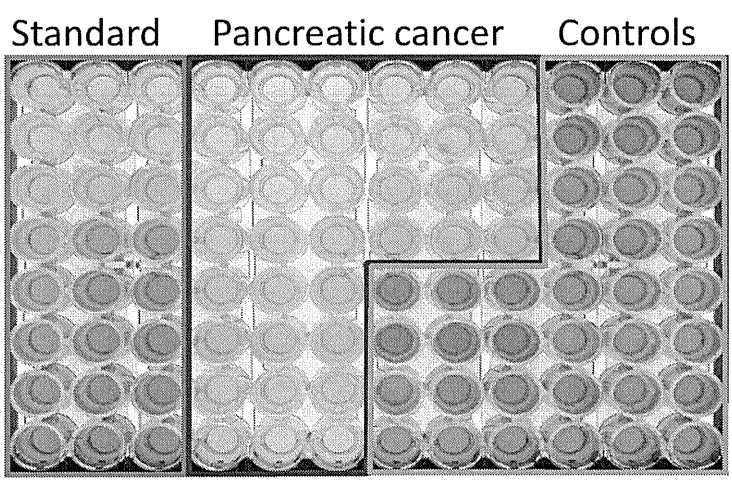

Supplementary Figure S7

A

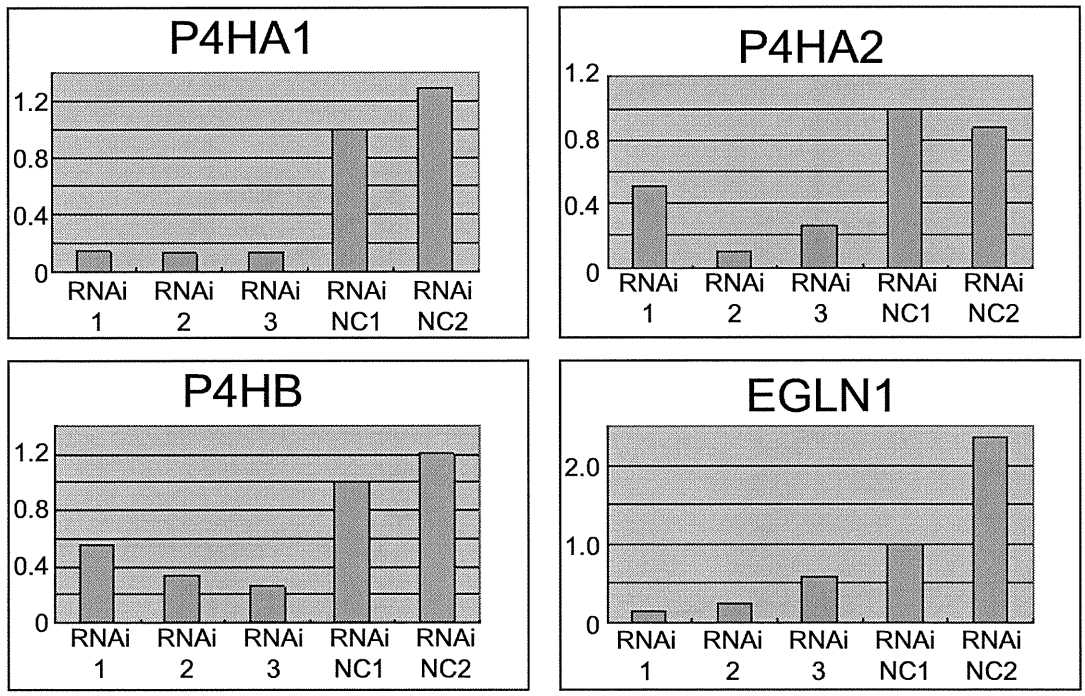

B

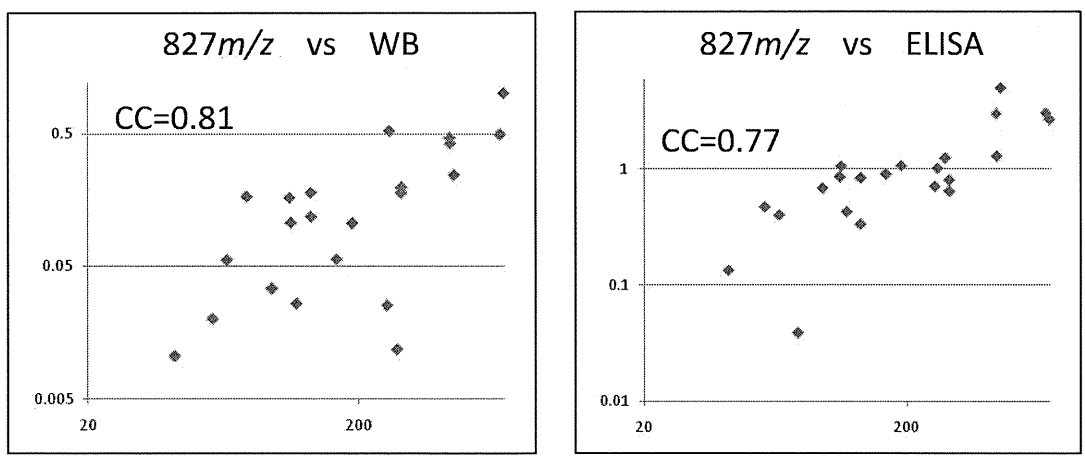

C

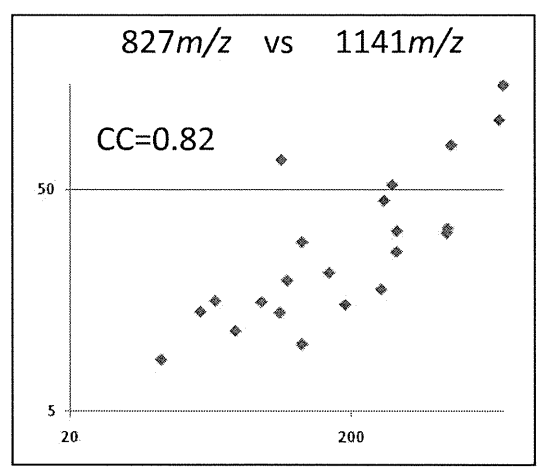

Supplementary Table S1

Intensity of peptide peaks that differed significantly between pancreatic cancer patients and healthy controls.

	Set 1 (18 cancer patients and 19 controls)			**Set 2** (20 cancer patients and 20 controls)		
Mass and RT	Control[1]	Cancer[1]	*P*-value[2]	Control[1]	Cancer[1]	*P*-value[2]
412 m/z, 13.7 min	35.3±18.2	14.1±8.6	7.02×10^{-6}	106.8±47.0	56.0±35.8	3.72×10^{-4}
546 m/z, 8.3 min	43.9±17.5	164.1±11.1	8.53×10^{-6}	32.4±17.5	88.2±62.3	7.94×10^{-5}
552 m/z, 8.3 min	147.4±92.6	457.3±304.8	2.35×10^{-4}	106.8±106.5	408.2±282.0	1.56×10^{-5}
827 m/z, 8.3 min	87.4±64.1	434.4±319.7	1.63×10^{-6}	73.7±81.5	282.9±228.4	4.19×10^{-4}
1141 m/z, 29.0 min	23.0±17.5	89.6±59.9	3.12×10^{-6}	17.3±12.2	52.6±49.7	3.27×10^{-4}
1185 m/z, 9.9 min	6.0±4.9	19.0±15.7	2.35×10^{-4}	8.3±4.9	25.1±19.1	1.04×10^{-4}

[1]Mean ± SD (in arbitrary unit determined by 2DICAL)

[2]Mann-Whitney *U* test (Control vs. Cancer)

Supplementary Table S2.

Plasma level of αFG-565HyP in pancreatic cancer patients with different stages.

		No. of cases	αFG-565HyP[1]	*P*-value[2]	CA19-9[3]	*P*-value[2]
Healthy control		113	0.91±1.24		11.5±11.1	
Pancreatic cancer	Total	160	2.26±2.28	3.80×10^{-15}	2117.9±3231.7	$<2.2\times10^{-16}$
	Stage IA[4]	2	1.10±1.45	0.8106	71.6±89.7	0.2106
	Stage IB[4]	4	3.43±3.81	0.02985	451.4±569.0	0.009444
	Stage IIA[4]	5	2.68±3.14	0.04045	174.5±190.4	0.001506
	Stage IIB[4]	28	2.15±2.39	3.067×10^{-5}	658.2±1079.6	2.404×10^{-13}
	Stage III[4]	41	1.93±1.71	3.392×10^{-7}	1963.0±3003.1	4.394×10^{-13}
	Stage IV[4]	78	2.42±2.43	1.878×10^{-12}	2897.2±3706.4	$<2.2\times10^{-16}$

[1]Mean ± SD (in arbitrary unit determined by competitive ELISA)

[2]Mann-Whitney *U* test (in comparison to "Healthy control")

[3]Mean ± SD (U/ml) measured with an immunoradiometric assay kit (Fujirebio Diagnostic, Malvern, PA)

[4]UICC stages (not available in 2 cases)

Supplementary Table S3.

Plasma level of αFG-565HyP in patients with different diseases.

	No. of cases	αFG-565HyP[1]	*P*-value[2]	CA19-9[3]	*P*-value[2]
Healthy control	113	0.91±1.24		11.5±11.1	
Pancreatic cancer	160	2.26±2.28	3.80×10^{-15}	2117.9±3231.7	$<2.2\times10^{-16}$
Chronic pancreatitis	12	1.30±0.74	0.03886	7.7±7.7	0.1504
Benign pancreatic tumor/cyst	37	1.12±1.31	0.2163	14.6±16.0	0.7751
Bile duct cancer	25	2.08±1.48	4.242×10^{-5}	961.8±2358.4	1.627×10^{-5}
Cholecystitis	22	0.51±0.53	0.1114	16.3±15.3	0.1939
Hepatocellular carcinoma	14	2.00±1.75	0.001077	61.6±167.9	0.1109
Esophageal cancer	10	1.96±0.77	0.0002065	17.7±14.2	0.07706
Gastric cancer	147	1.30±1.38	0.0005951	137.8±932.4	0.01655
Colorectal cancer	145	1.60±1.82	9.287×10^{-6}	75.2±357.7	0.00779

[1]Mean ± SD (in arbitrary unit determined by competitive ELISA)

[2]Mann-Whitney *U* test (in comparison to "Healthy control")

[3]Mean ± SD (U/ml)

Hindawi Publishing Corporation
International Journal of Proteomics
Volume 2011, Article ID 739615, 11 pages
doi:10.1155/2011/739615

Research Article

Combined Use of a Solid-Phase Hexapeptide Ligand Library with Liquid Chromatography and Two-Dimensional Difference Gel Electrophoresis for Intact Plasma Proteomics

Tatsuo Hagiwara,[1,2] Yumi Saito,[1] Yukiko Nakamura,[1,3] Takeshi Tomonaga,[3] Yasufumi Murakami,[2] and Tadashi Kondo[1]

[1] *Division of Pharmacoproteomics, National Cancer Center Research Institute, Chuo-ku, Tokyo 104-0045, Japan*
[2] *Laboratory of Genome Biology, Department of Biological Science and Technology, Tokyo University of Science, Tokyo 278-8510, Japan*
[3] *Laboratory of Proteome Research, National Institute of Biomedical Innovation, Osaka 567-0085, Japan*

Correspondence should be addressed to Tadashi Kondo, takondo@ncc.go.jp

Received 2 May 2011; Accepted 9 June 2011

Academic Editor: David E. Misek

The intact plasma proteome is of great interest in biomarker studies because intact proteins reflect posttranslational protein processing such as phosphorylation that may correspond to disease status. We examined the utility of a solid-phase hexapeptide ligand library in combination with conventional plasma proteomics modalities for comprehensive profiling of intact plasma proteins. Plasma proteins were sequentially fractionated using depletion columns for albumin and immunoglobulin, and separated using an anion-exchange column. Proteins in each fraction were treated with a solid-phase hexapeptide ligand library and compared to those without treatment. Two-dimensional difference gel electrophoresis demonstrated an increased number of protein spots in the treated samples. Mass spectrometric studies of these protein spots with unique intensity in the treated samples resulted in the identification of high- and medium-abundance proteins. Our results demonstrated the possible utility of a solid-phase hexapeptide ligand library to reveal greater number of intact plasma proteins. The characteristics of proteins with unique affinity to the library remain to be clarified by more extensive mass spectrometric protein identification, and optimized protocols should be established for large-scale plasma biomarker studies.

1. Introduction

The plasma proteome has been extensively investigated with the aim of biomarker development [1, 2]. Plasma is the most accessible clinical material, and plasma biomarkers for early diagnosis and monitoring the response to therapy and disease recurrence would be beneficial for patients with cancer. Because proteins released by tumors, particularly early-stage tumors, are expected to exist in very low concentrations and plasma contains various proteins with considerable heterogeneity between and within patients, the identification of novel plasma biomarkers represents a substantial challenge.

Global expression studies on intact plasma proteins are of special interest in biomarker studies as the intact proteins reflect the functional features of protein structure. Those include posttranslational processing such as phosphorylation and glycosylation. Peptide subsets from complex digests have been analyzed for plasma proteomics, resulting in the identification of low-abundance proteins such as tissue leakage proteins [3] and biomarker candidates [4]. However, analysis of peptide digests may not be sensitive to posttranslational protein processing, and may therefore not reveal many relevant protein isoforms associated with disease status. To date, much effort has been devoted to detect trace intact proteins in complex plasma samples.

The utility of a combinatorial hexapeptide ligand library immobilized on a solid-phase matrix has been reported, introduced to intact plasma proteomics [5–9], and

commercialized as ProteoMiner (Bio-Rad Laboratories, Hercules, CA, USA). ProteoMiner contains millions of randomly synthesized hexapeptide ligands that are equally represented with a selected number of targets. When a complex plasma protein extract is exposed, the hexapeptide ligands for high-abundance proteins are saturated, but the majority remains unbound. In contrast, the proteins which do not saturate the corresponding hexapeptide ligands and usually not observed by the conventional methods will appear in the proteome data. The approach of using a combinatorial hexapeptide ligand library is different from that of using depletion and separation; thus, it reveals a novel aspect of the plasma proteome. A recent report demonstrated that prefractionation using a hexapeptide ligand library for shotgun mass spectrometry studies identified plasma proteins not recorded in the Human Plasma Proteome Project [10]. The combined use of a hexapeptide ligand library with depletion and separation methods has also been a challenge in deeper plasma proteomics [11], and the resulting protein contents are examined by gel electrophoresis and mass spectrometry [12, 13]. ProteoMiner has been used for disease biomarker studies in lung cancer [14] and liver cancer [15]. Considering that it will potentially visualize the unique plasma proteome aspects, the application and optimization of a solid-phase hexapeptide ligand library for disease biomarker studies should be further investigated.

In this study, we examined the utility of a solid-phase hexapeptide ligand library in combination with a depletion column, an anion-exchange column, and 2D-DIGE that allows an instant visual comparison of the protein patterns. Protein spots exhibiting prominent differences between samples treated with and without the library were subjected to mass spectrometry. Our study clearly demonstrated that the combined use of the ProteoMiner and the other proteomics modalities can visualize unique plasma proteome.

2. Materials and Methods

2.1. Sample Preparation. Frozen human plasma was purchased from Cosmobio KOJ (Tokyo, Japan). After the plasma was placed on ice, 40 mL plasma was centrifuged and 30 mL supernatant was recovered for the following experiments.

2.2. Albumin Depletion. Albumin and other proteins were separated using a HiTrap Blue HP column (5 mL resin, GE, Uppsala, Sweden) with the AKTA Explorer system (GE) at a flow rate of 1.0 mL/min. The separation was initiated by washing the column with rinse buffer (50 mM KH_2PO_4/Na_2HPO_4, pH 7.0) for 5 min. Plasma (30 mL) was diluted with 60 mL 50 mM KH_2PO_4/Na_2HPO_4 (pH 7.0), and 9 mL of the diluted plasma was injected. The column was then washed with binding buffer (50 mM KH_2PO_4/Na_2HPO_4, pH 7.0) for 35 min, and the flow-through fraction was collected. Bound proteins were eluted from the column with elution buffer (50 mM $KHPO_4$, 1.5 M KCl, pH 7.0) for 45 min, and the bound fraction was collected. The column was neutralized with rinse buffer for 20 min. This process was repeated 10 times for a total of 90 mL of diluted plasma.

One-third of the flow-through and bound fractions, approximately 150 mL of each, was concentrated to 1.2 mL using a VIVA Spin 20 column (10 K MWCO, 20 mL capacity, Sartorius, Gotteingen, Germany). Then, 1.0 mL and 0.20 mL of the concentrated samples were subjected to treatment with the solid-phase hexapeptide ligand library and 2D-DIGE, respectively. Two-thirds of the flow-through fraction, approximately 300 mL, was subjected to an immunodepletion column.

2.3. Immunoglobulin Depletion. Immunoglobulin was depleted using the HiTrap Protein G HP column (1 mL resin, GE) with the AKTA Explorer system (GE) at a flow rate of 1.0 mL/min. The depletion was initiated by washing the column with rinse buffer (50 mM KH_2PO_4/Na_2HPO_4, pH 7.0) for 4 min. After 15 mL of the flow-through fraction from the HiTrap Blue HP column was injected, the column was washed with binding buffer (50 mM KH_2PO_4/Na_2HPO_4, pH 7.0) for 5 min, and the flow-through fraction was collected. Bound proteins were eluted from the column with elution buffer (0.1 M glycine-HCl, pH 2.2) for 8 min and collected as the bound fraction. The collected bound fraction was immediately neutralized with neutralizing buffer (1.0 M Tris-HCl, pH 9.0). The column was equilibrated with rinse buffer for 5 min for reuse. This process was repeated 20 times for a total of two-thirds of the flow-through fraction from the HiTrap Blue HP column (approximately 300 mL).

Half of the flow-through and bound fractions (approximately 200 mL and 80 mL, resp.) were concentrated to 1.2 mL and 0.25 mL, respectively, using VIVA Spin 20 columns (Sartorius). Then, 1.0 mL of the concentrated flow-through fraction and 0.20 mL of the concentrated bound fraction were subjected to treatment with the solid-phase ligand library, and the remaining samples were subjected to 2D-DIGE. Another half of the flow-through fraction (approximately 200 mL) was concentrated to 2.0 mL using the VIVA Spin 20 column (Sartorius). After diluting with 38 mL of 25 mM Tris-HCl (pH 9.0), the sample was subjected to separation on an anion-exchange column.

2.4. Anion Exchange. The flow-through fraction from the HiTrap Protein G HP column was separated using the Resource Q column (1 mL resin, 6.4 mm id × 30 mm, GE) with the AKTA Explorer system (GE) at a flow rate of 3.0 mL/min. The separation was initiated by washing the column with rinse buffer (25 mM Tris-HCl, pH 9.0) for 4 min, and 5 mL of the flow-through fraction from the HiTrap Protein G HP column was injected. The separations were performed using a stepwise NaCl gradient as follows: 0, 100, 150, 200, 250, and 1000 mM for 5 min each. All samples contained 25 mM Tris-HCl, pH 9.0. The column was washed with rinse buffer (25 mM Tris-HCl, pH 9.0) for 5 min. This process was repeated 8 times for a total of 40 mL of the diluted flow-through fraction from the HiTrap Protein G HP column.

The collected samples were concentrated to 0.25 mL, and the buffer was exchanged gradually with 25 mM Tris-HCl (pH 9.0) using the VIVA Spin 20 column (Sartorius). Then,

0.2 mL and 0.05 mL were subjected to treatment with the solid-phase ligand library and 2D-DIGE, respectively.

2.5. Treatment with the Solid-Phase Ligand Library. A solid-phase combinatorial library of hexapeptides was purchased from Bio-Rad Laboratories (ProteoMiner kit). Unprocessed plasma (1 mL) and the flow-through fractions from the HiTrap Blue HP and HiTrap Protein G HP columns were treated using the ProteoMiner large-capacity kit, and 0.2 mL of the bound fraction from the HiTrap Protein G HP column, and all fractions from the Resource Q column were treated using the ProteoMiner small-capacity kit. After 2 h of incubation at room temperature, the unbound fraction was washed out by centrifugation. After rinsing, the bound sample was eluted with an elution reagent containing 8 M urea, 2% CHAPS, and 5% acetic acid, according to the manufacturer's instructions.

2.6. Measurement of Protein Concentration. Protein concentration was measured using a protein assay kit (Bio-Rad), according to the manufacturer's instructions (Table 1).

2.7. SDS-PAGE. Protein samples (1 μg) were examined by electrophoresis using 18-well precast 12.5% polyacrylamide gel plates (e-PAGEL, ATTO, Tokyo, Japan). Electrophoresis was performed at a constant current of 40 mA for 80 min and using the page Run AE6531 system [16]. Silver staining was performed using the Silver Stain KANTO III kit (Kanto Chemical, Tokyo, Japan), according to the manufacturer's instructions.

2.8. 2D-DIGE. 2D-DIGE was performed as described previously [17]. Briefly, protein samples (20 μg) were labeled with the Cy3 or Cy5 fluorescent dye (CyDye DIGE Fluor saturation dye, GE), and differentially labeled protein samples were mixed. After dividing into 3, the labeled protein samples were separated by 2D-PAGE. The first-dimension separation was performed using a 24 cm length immobiline gel (IPG, pI 4–7, GE) and Multiphor II (GE) whereas the second-dimension separation was performed using gradient gels prepared in house and EttanDalttwelve (GE). The gels were scanned using a laser scanner (Typhoon Trio, GE) at an appropriate wavelength for Cy3 or Cy5. The Cy3 and Cy5 intensities were compared in the same gel using the Progenesis SameSpots software (version 4.0; Nonlinear Dynamics, Newcastle, UK). ProteoMiner-treated and untreated samples were labeled with Cy3 and Cy5, respectively, or with Cy5 and Cy3, respectively. Six gels were run for each sample. The average value of the intensity ratio was calculated among the triplicate gels for all protein spots and then averaged between the 2 samples for further study. Spot intensity data were exported from the Progenesis SameSpots software as Excel files amenable to numerical data analysis.

2.9. Mass Spectrometric Protein Identification. Proteins were extracted from the protein spots by in-gel digestion, as reported previously [17]. Briefly, protein samples (100 μg) were labeled with Cy3 and separated by 2D-PAGE. The protein spots were then recovered from the gel pieces using an automated spot recovery machine. The recovered protein spots were extensively washed with a solution containing acetonitrile and ammonium bicarbonate minimum and treated with trypsin (Promega, Madison, WI, USA) at 37°C overnight. The tryptic digests were recovered from the gel pieces, concentrated by vacuum, and resolubilized with 0.1% trifluoroacetic acid. The final tryptic digests were subjected to mass spectrometry, which was performed using the LXQ linear ion trap mass spectrometer (Thermo Electron, San Jose, CA, USA). The Mascot software (version 2.3.0; Matrix Science, London, UK) was used to search for the mass of the peptide ion peaks against the SWISS-PROT database (Homo sapiens, 471472 sequences in Sprot_57.5 fasta file). The search parameters were as follows: trypsin digestion allowing up to 3 missed tryptic cleavages, fixed modifications of

TABLE 1: List of the identified proteins and their reported concentration.

Protein name	Normal concentration μg/mL
Adiponectin	2–17
Albumin	35000–52000
Alpha-1-antitrypsin	900–2000
Alpha-1B-glycoprotein	150–300
Alpha-2-macroglobulin	1300–3000
Apolipoprotein A-I	1000–2000
Apolipoprotein A-II	190–300
Apolipoprotein A-IV	110–220
Apolipoprotein D	60–90
Apolipoprotein E	30–60
Carboxypeptidase N	30
Ceruloplasmin	190–370
Clusterin	250–420
Coagulation factor X	10
Complement C3	900–1800
Complement C4-A	25–90
Fibrinogen beta chain	520–1420
Fibrinogen gamma chain	490–1340
Ficolin-2	1–12
Ficolin-3	3–54
Haptoglobin	200–2000
Haptoglobin-related protein	32–41
Inter-alpha-trypsin inhibitor (heavy chain H3)	100–200
Paraoxonase/arylesterase 1	58–61
Prothrombin	100
Serotransferrin	2000–3600
Transthyretin	200–400
Vitronectin	240–530
Zinc-alpha-2-glycoprotein	60–80

The table with the references for the protein concentration is shown in Supplementary Table 7 in Supplemrntary material available online at doi: 10.1155/2011/39615.

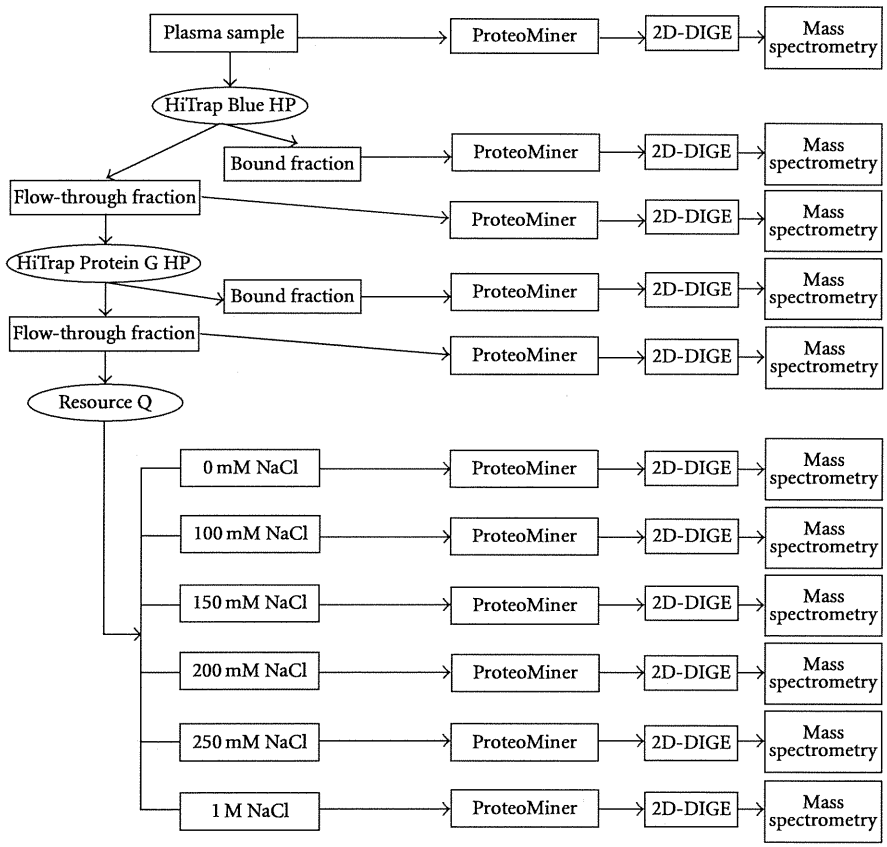

FIGURE 1: Overview of protein fractionation by sequential use of 3 different columns to separate plasma proteins. All fractions were subjected to ProteoMiner and 2D-DIGE.

carbamidomethyl, variable modifications of oxidation, 1^+, 2^+, and 3^+ peptide charge, peptide mass tolerance of 2.0 Da, and use of MS/MS tolerance of 1.0 Da for all tryptic-mass searches.

3. Results and Discussion

We previously reported the utility of combining multidimensional chromatography and 2D-DIGE for intact plasma proteomics. Extensive fractionation by the different separation modes increased the number of protein spots on 2D-DIGE and allowed a quantitative comparison between the plasma samples from healthy donors and those from patients with lung adenocarcinoma [18] and pancreatic cancer [19]. However, mass spectrometric protein identification revealed that protein spots with a significant difference between the sample groups corresponded to high- and medium-abundance proteins such as acute-phase proteins, but no known plasma tumor markers were detected. Thus, we concluded that further investigations are needed to reveal low-abundance proteins for biomarker studies. In this study, we examined whether a novel technology, a solid-phase hexapeptide ligand library could improve the linkage of multidimensional chromatography and 2D-DIGE.

3.1. Overall View of Protein Fractionation: Comparison and Detection. The overall view of sequential protein separation is shown in Figure 1. A sample equivalent to 10 mL plasma was separated using 3 different columns and then treated with the solid-phase hexapeptide ligand library ProteoMiner. The ProteoMiner-treated and untreated samples were compared using 2D-DIGE by labeling them with different fluorescent dyes and separating the labeled proteins on an identical gel. The protein spots with significantly different intensities between the ProteoMiner-treated and untreated samples were subjected to mass spectrometry to identify the proteins.

The number of observable low-abundance proteins was affected by the initial amount of plasma sample and the sensitivity of the final quantification method. We used a relatively large volume of plasma sample (10 mL) as the initial material. The immunodepletion columns allow the use of only a small volume of plasma sample for separation. Furthermore, a significantly larger number of plasma samples should be examined to obtain conclusive results for biomarker development. A larger volume of samples can be manipulated by repeatedly using the same immunodepletion column. Although it is quite feasible, special attention may be required to maintain reproducibility during a long period of use. In this study, we used Blue Sepharose and Protein

G-Sepharose columns in a sequential manner to deplete albumin and subsequently immunoglobulin and to minimize repeated use of the same column. Although these columns may have less sensitivity than an immunodepletion column and deplete nontargeted proteins that may bind to albumin and immunoglobulin, a larger volume of plasma sample can be treated in individual procedures. A previous study indicated that Cibacron Blue beads remove a major portion of the albumin but with concomitant loss of potentially important peptides and proteins [20]. Thus, we examined both the column-bound and flow-through fractions (Figure 1). Although the specificity of Cibacron Blue beads was not validated in this study, as the purpose of Cibacron Blue was to reduce the complexity of plasma sample, it should not be problem.

To avoid possible redundant proteins in the neighboring fractions as much as possible when utilizing the anion-exchange column, we used stepwise elution and fractionation; once all proteins were eluted, the next elution buffer was applied to the column (Figure 1). Considering the complexity of the samples and resolution of an anion-exchange column, extensive fractionation with a gradient buffer system may result in redundant contents among the fractions. We employed 6 stepwise fractionations by monitoring the fraction contents using SDS-PAGE (data not shown).

3.2. High Reproducibility of Protein Fractionation by Chromatography. The ultraviolet detection (280 nm) trace for each run demonstrated consistent separation of albumin and immunoglobulin from the depletion and anion-exchange columns. This high reproducibility may suggest the possible utilities of this approach for biomarker studies (Supplementary Figure 1). High quantitative and qualitative reproducibility of the solid-phase hexapeptide ligand library ProteoMiner has been confirmed in previous reports [21, 22].

3.3. Demonstration of the Effects of Fractionation and Dynamic Range Reduction. We examined the effects of sequential plasma protein fractionation using 3 columns and the reduction of dynamic range by ProteoMiner (Figure 2). The contents of the fractionated samples were apparently different from each other. Notably, the protein sample bound to the Blue Sepharose and Protein G-Sepharose columns included many proteins that should be different from the targeted proteins, according to their molecular weights. Treatment of the fractionated samples with ProteoMiner enhanced the proteins that were not observed, except for those bound to the Protein G-Sepharose column. Treatment of the bound fraction from the Protein G-Sepharose column with ProteoMiner did not result in a greater number of observable proteins. This may have been due to the low complexity and narrow dynamic range of proteins in the bound fraction from the Protein G-Sepharose column. There was one order of magnitude in concentration difference for the observed protein bands in the ProteoMiner-treated sample. These observations may reflect that the affinity of proteins for the peptide may not be equal and even the number of peptides bound on the beads is equal, the amount of proteins bound to the ProteoMiner may be different

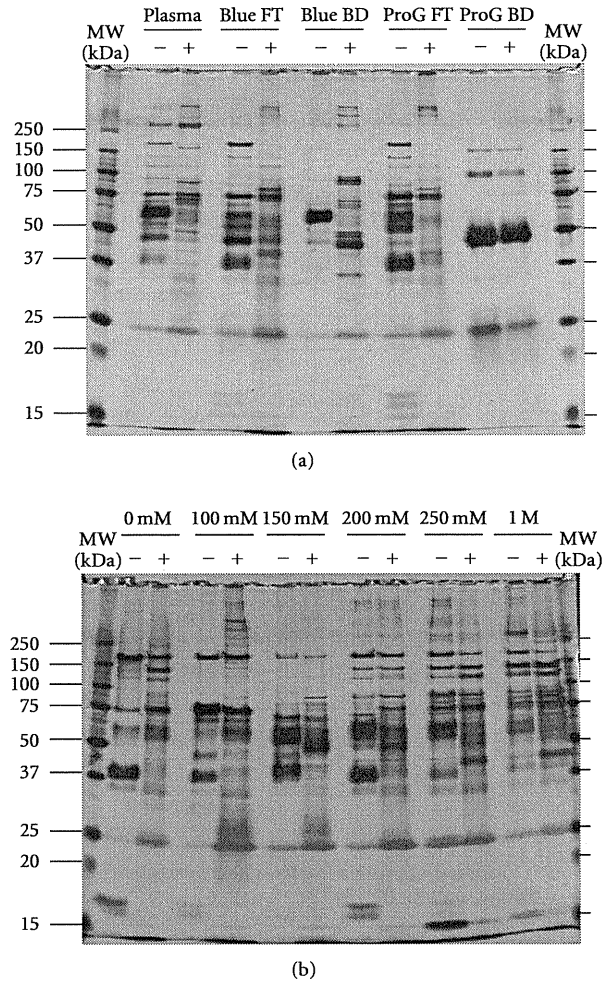

FIGURE 2: Overview of the protein contents fractionated by liquid chromatography and ProteoMiner. The fractionated protein samples were loaded onto SDS-PAGE, and the protein contents were visualized by silver staining.

depending on their affinity. This fraction contained similar amounts of only 4 major proteins, as revealed by SDS-PAGE (Figure 2), and they may have been absorbed to ProteoMiner in proportion to their original amount.

The concentration and amount of protein samples before and after ProteoMiner treatment are summarized in Supplementary Table 1. The recovery rate from ProteoMiner was between 0.54 and 6.33%, suggesting that a unique population of protein species selectively bound to ProteoMiner. This assumption was supported by the SDS-PAGE data, except the bound fraction from the Protein G-Sepharose column which included only 4 major proteins that were bound to ProteoMiner (Figure 2).

3.4. Higher Separation of Fractionated Protein Samples and an Evaluation of the Effects of ProteoMiner Treatment. Although SDS-PAGE separated individual proteins with higher

resolution than chromatography in this study, using it for a quantitative comparison in a biomarker study may be troublesome because many protein bands obviously overlapped (Figure 2). Thus, we subjected the fractionated samples to 2D-DIGE in order to separate the proteins with higher resolution. Bandow compared ProteoMiner-treated and untreated plasma samples using conventional 2D-PAGE and demonstrated substantial differences between unprocessed and immunodepleted plasma samples [11]. In 2D-DIGE, 2 protein samples were labeled with different fluorescent dyes, mixed, and separated by 2D-PAGE. Because the 2 samples were separated on an identical 2D-PAGE, gel-to-gel variation was compensated. In addition, the wide dynamic range of the fluorescent dyes enabled a quantitative comparison. 2D-DIGE has been applied to compare the performance of ProteoMiner with an immunodepletion column [12]. We further extended the evaluation of the utility of ProteoMiner by loading a high amount of protein and examining the proteins separated by an anion-exchange column.

The fluorescent 2D-PAGE images of the ProteoMiner-treated and untreated samples were overlaid with different colors, so that the unique protein contents were visualized (Figures 3 and 4). The results of experiments in which the fluorescent dyes were swapped are shown in Supplementary Figure 2. Consistent with the SDS-PAGE results (Figure 2), Figure 3 demonstrates that the approach involving depletion of high-abundance proteins and multidimensional separation was an effective prefractionation method to increase the number of protein spots, and the use of ProteoMiner treatment also contributed to reveal more plasma proteins. Because these fractionation methods are based on different binding properties of proteins, their combined use revealed additional plasma proteins.

The number of observed protein spots on 2D gel electrophoresis is summarized in Supplementary Table 2. Overall, the total number of protein spots increased by treating the samples with ProteoMiner, except for the bound fraction from the Protein G-Sepharose column. This observation suggests that ProteoMiner may be a useful tool to observe a greater number of protein spots in prefractionated samples.

We compared the protein spots of the samples with and without ProteoMiner treatment (Supplementary Table 3). Depending on the criteria, different numbers of protein spots showed significantly different intensities. Although the total number of protein spots increased by treating the samples with ProteoMiner (Supplementary Table 2), many protein spots revealed decreased intensity with treatment, suggesting the selective enrichment by ProteoMiner.

3.5. Mass Spectrometric Identification of Proteins with Different Affinities to ProteoMiner. To reveal the characteristics of proteins with a particularly high or low affinity to ProteoMiner, among the protein spots with greater than 5-fold differences (Supplementary Table 3), we selected those with the top 10% different intensities between the ProteoMiner-treated and untreated samples in each fraction and subjected them to mass spectrometric identification. A total of 200 protein spots were subjected to mass spectrometry, and a positive identification was obtained for 128 (Supplementary Table 4). A list of the identified proteins is provided in Supplementary Table 5, and data supporting protein identification are shown in Supplementary Table 6. These 128 protein spots corresponded to 29 unique proteins. Because the fold difference of the protein spots in the bound fraction from the Protein G-Sepharose column was less than 4, we did not examine them. Of the original plasma samples, vitronectin and albumin were most affected by ProteoMiner treatment and disappeared after depletion and fractionation using the anion-exchange column. The other proteins were identified as enriched (or nonenriched) by ProteoMiner treatment. Proteins bound to ProteoMiner have been reported in previous studies in which the proteins were globally identified by mass spectrometry. Dwivedi et al. demonstrated that albumin, alpha 1-antitrypsin, alpha 2-macroglobulin, apolipoprotein A-I, apolipoprotein A-II, haptoglobin-related protein, and serotransferrin have high affinity to ProteoMiner [21]. In addition, Beseme et al. identified apolipoprotein A-IV, apolipoprotein D, apolipoprotein E, ceruloplasmin, complement C3, fibrinogen beta, fibrinogen gamma, ficolin-2, ficolin-3, paroxonase I, prothrombin, transthyretin, and vitronectin [23]. The protein concentrations identified in this study are summarized in Supplementary Table 6. According to the literatures, the identified proteins were classified as high- and medium-abundance proteins. Adiponectin and the carboxypeptidase N catalytic chain are not reported in previous studies, in which ProteoMiner-treated samples were examined by 2D-PAGE and mass spectrometry.

Adiponectin is an adipocytokine [24–27] and plays a protective role against obesity-related disorders such as metabolic syndrome [28], type 2 diabetes [29], and cardiovascular disease [30]. Low levels of plasma adiponectin are associated with obesity [31] and many types of malignancies such as liver cancer [32], breast cancer [33], pancreatic cancer [34], and endometrial cancer [35]. An epidemiological study suggested that adiponectin is involved in early colorectal carcinogenesis [36], and that a low circulating adiponectin level is correlated with a poor prognosis in patients with colorectal cancer [37]. The molecular backgrounds of these observations may be attributable to the antiproliferative effects of adiponectin on cancer cells [38].

Carboxypeptidase N (CPN), which is also known as kininase I, arginine carboxypeptidase, and anaphylatoxin inactivator, is a zinc finger metalloprotease. It cleaves basic lysine and arginine residues from the carboxy terminal of proteins [39]. CPN is produced in the liver and secreted into the plasma. It modulates the activity of cytokines such as stromal cell-derived factor-1 alpha [40]. The association of CPN1 with malignancy and other diseases has not been reported, and the clinical utility of CPN1 has not been suggested.

The working hypothesis of this study was that the combined use of different separation methods, including a solid-phase hexapeptide ligand library, would increase the number of observable proteins, and finally visualize the proteome that may not be observed otherwise. By loading a high amount of protein and using extensive prefractionation techniques prior to using ProteoMiner, trace proteins became visible in SDS-PAGE, and the number of protein spots on

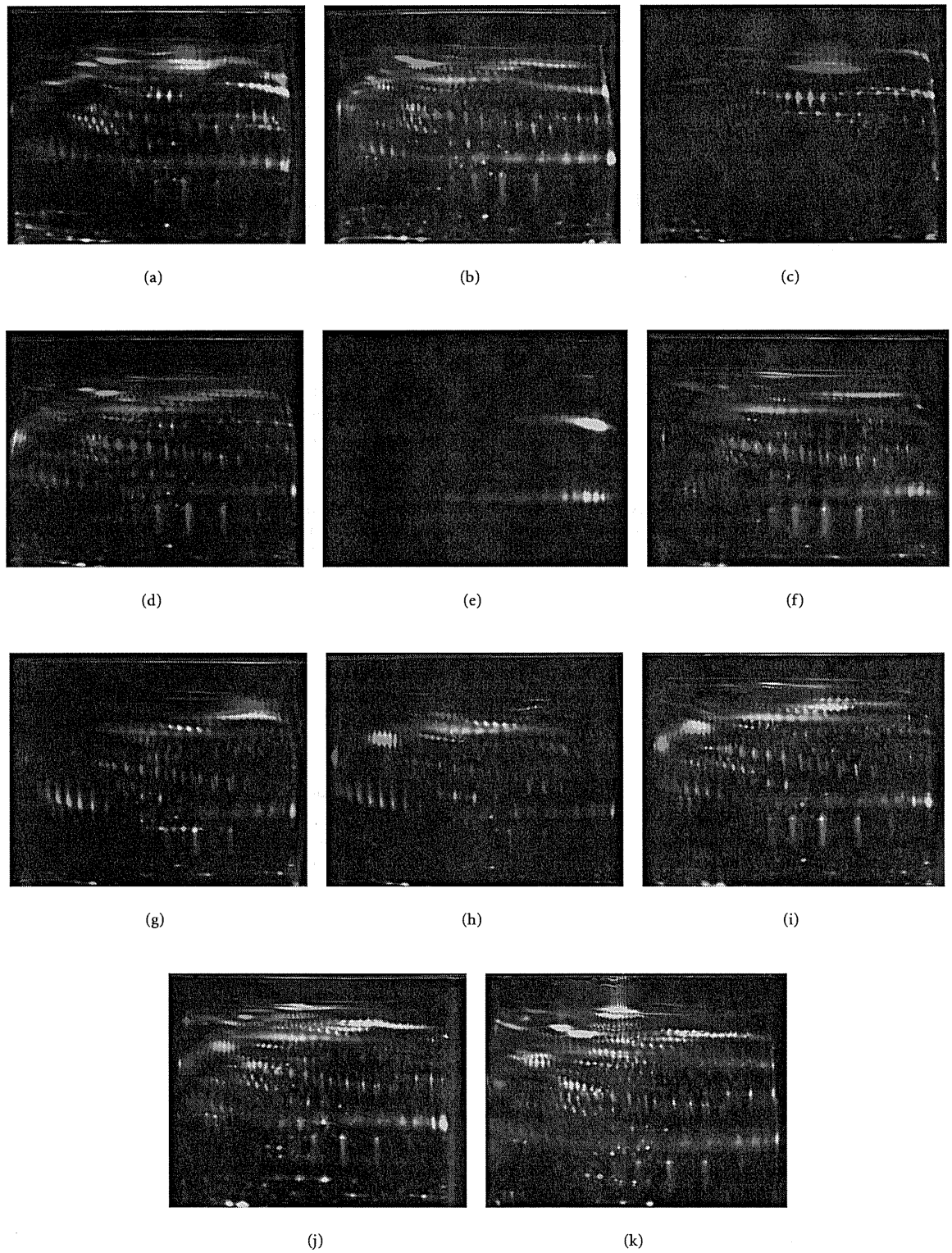

FIGURE 3: Effects of ProteoMiner treatment were examined by 2D-DIGE. The ProteoMiner-treated and untreated samples were labeled with Cy3 and Cy5, respectively, mixed, and separated by 2D gel electrophoresis. Note that a significant number of protein spots showed different intensities between the 2 samples. The dye-swapped images are shown in Supplementary Figure 2. (a) Original plasma; (b) flow-through fraction of HiTrap Blue HP column; (c) binding fraction of HiTrap Blue HP column. (d) Flow-through fraction of HiTrap Protein G HP column. (e) Binding fraction of HiTrap Protein G HP column; 0 mM fraction. (f) 100 mM fraction. (g) 150 mM. (h) 200 mM. (i) 250 mM. (j) 1 M fraction. (k) Resource Q column.

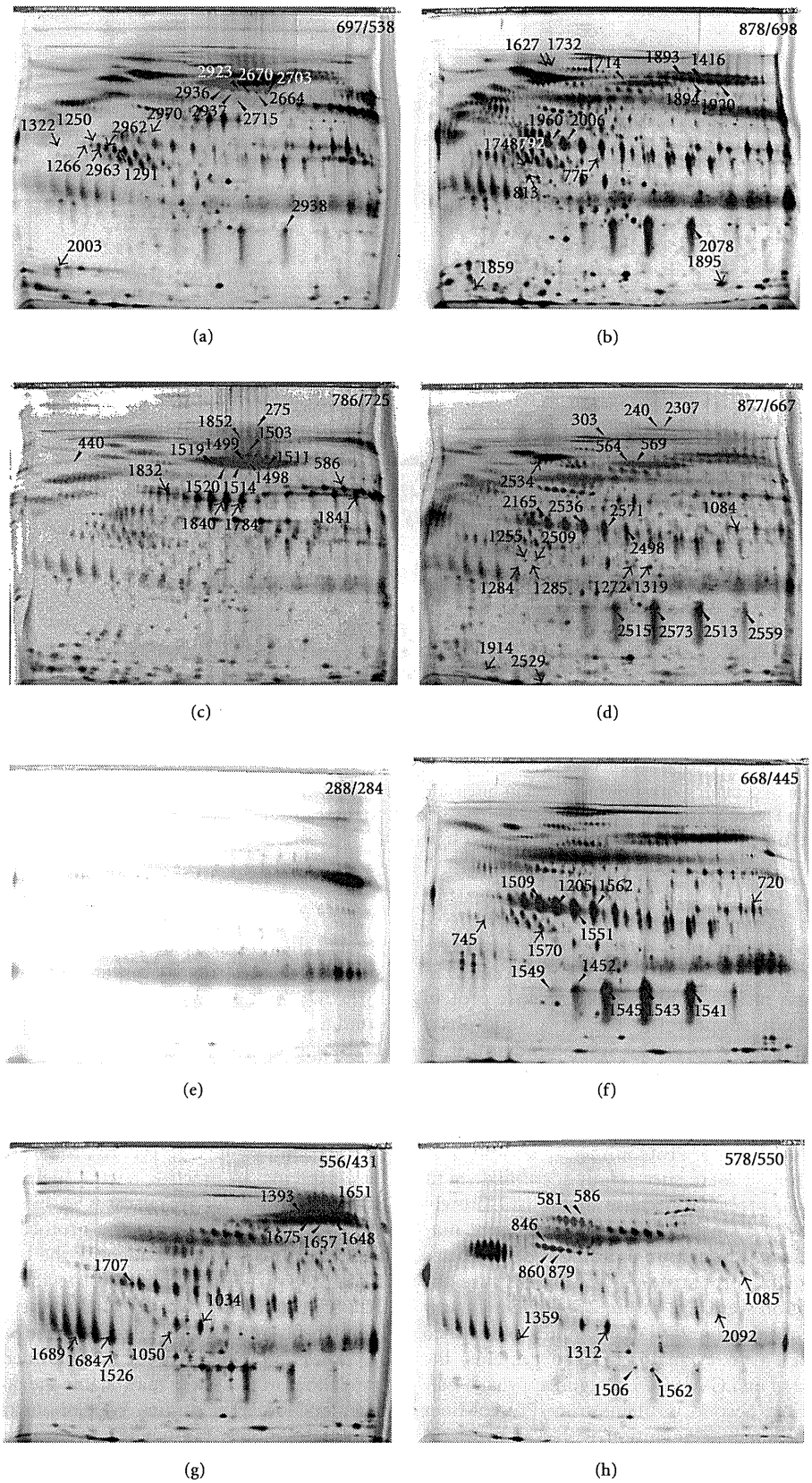

FIGURE 4: Continued.

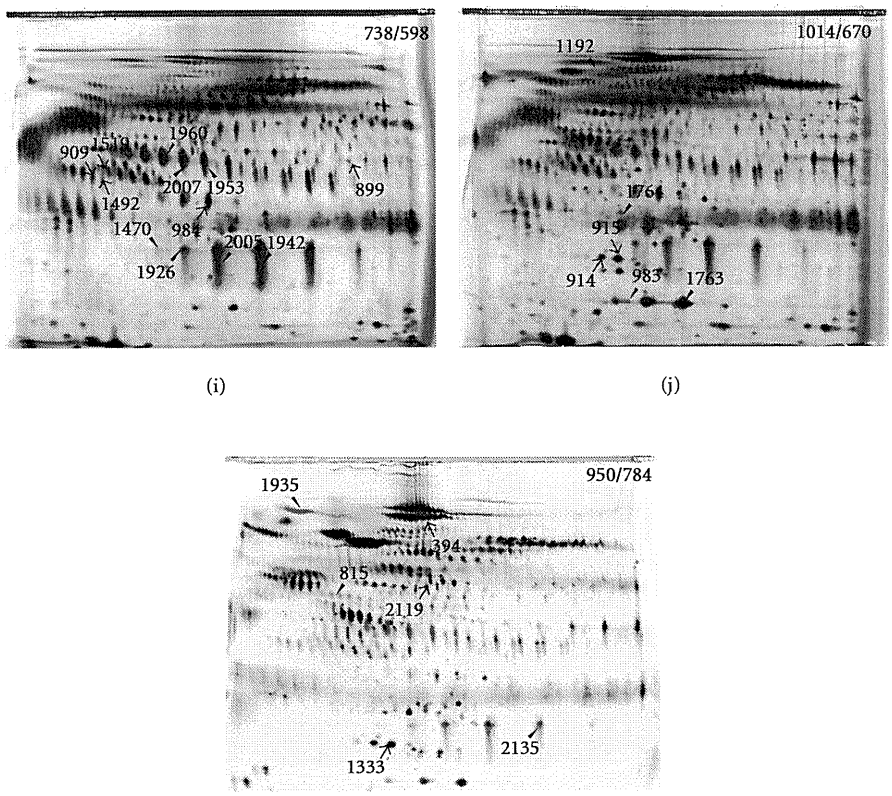

FIGURE 4: Localization of protein spots showing different intensities between the ProteoMinor-treated and untreated samples. Panels (a–k) correspond to those in Figure 3. The protein spot numbers corresponds to those in Supplementary Tables 5 and 6. −/−: number of protein spots without ProteoMiner treatment/those with ProteoMiner treatment.

2D-DIGE increased significantly. This approach may pave a way to a novel strategy for intact plasma proteomics. In contrast, the present results of mass spectrometric protein identification did not support the use of a solid-phase hexapeptide ligand library to enrich low-abundance proteins. It may be because our present approach had 3 limitations. First, mass spectrometric identification was performed for proteins with a greater prominent difference between the samples with or without ProteoMiner treatment, and only 128 of 200 proteins were successfully identified (Supplementary Table 4), probably because of the low protein amount. Proteins with a smaller difference or amount may include trace proteins. Although we optimized the protocols for mass spectrometric protein identification because the sensitivity of the fluorescent dye in the 2D-DIGE was very high, not all protein spots on 2D-DIGE could be identified by mass spectrometry. To evaluate enriched proteins, the complementary use of an LC-MS/MS shotgun approach may be worth considering. Second, proteins from ProteoMiner were recovered by a single-step elution with 8 M urea, 2% CHAPS, and 5% acetic acid, according to the manufacturer's instructions (Bio-Rad). However, because proteins may have interacted with hexapeptide ligand libraries in all possible modes, the absolute elution process may require sequential steps or more stringent buffer conditions such as boiling 10% SDS with 3% DTE [41]. Furthermore, various binding conditions may also be worth considering to capture whole binding proteins [9]. Third, considering the practical use of trace proteins in a biomarker study, we used as much sample as possible for identifying them and examined 10 mL plasma samples as an initial source. However, a larger volume of plasma sample, such as 100 mL, might be needed to collect rare proteins. In practice, such a high volume of plasma is rarely obtained for many cases in biomarker studies, and we may need to optimize the protocols for use of 10 mL plasma. For instance, we identify the biomarker candidates using 100 mL plasma, and using specific antibody against the identified candidate, we will be able to screen a relatively large number of samples with 10 mL volume or less.

The combined use of the ProteoMiner and the proteomic modalities in this study may enable the quantitative comparison for biomarker studies. We demonstrated that the liquid chromatography was quantitatively reproducible (Supplementary Figure 1), and the quantitative reproducibility of the ProteoMiner and 2D-DIGE was previously reported [10, 17]. We may further need to examine how the combined

use of such reproducible methods generate the results in a reproducible way, considering the degree of differences that we expect between the samples to be compared.

4. Conclusions

The use of ProteoMiner in combination with conventional proteomic modalities such as depletion and anion-exchange columns significantly enhanced trace proteins on SDS-PAGE and increased the number of protein spots on 2D-DIGE, suggesting that the use of a solid-phase hexapeptide ligand library has great potential for intact plasma proteomics. Mass spectrometric protein identification revealed that high- and middle-abundance proteins were enriched by ProteoMiner, and the characteristics of proteins with unique affinity to a solid-phase hexapeptide ligand library remain to be clarified by more extensive mass spectrometric protein identification. Although use of ProteoMiner for biomarker studies is quite feasible and attractive, more extensive characterization of binding proteins and optimized protocols are required for large-scale biomarker studies.

Acknowledgments

This paper was supported by the Ministry of Health, Labor, and Welfare and by the Program for Promotion of Fundamental Studies in Health Sciences of the Organization for Pharmaceutical Safety and Research of Japan, T. Kondo was a principal funding recipient. The authors report no conflicts of interests.

References

[1] S. M. Hanash, S. J. Pitteri, and V. M. Faca, "Mining the plasma proteome for cancer biomarkers," *Nature*, vol. 452, no. 7187, pp. 571–579, 2008.

[2] Z. Zhang and D. W. Chan, "The road from discovery to clinical diagnostics: lessons learned from the first FDA-cleared in vitro diagnostic multivariate index assay of proteomic biomarkers," *Cancer Epidemiology Biomarkers and Prevention*, vol. 19, no. 12, pp. 2995–2999, 2010.

[3] H. Zhang, A. Y. Liu, P. Loriaux et al., "Mass spectrometric detection of tissue proteins in plasma," *Molecular and Cellular Proteomics*, vol. 6, no. 1, pp. 64–71, 2007.

[4] Q. Zhang, V. Faca, and S. Hanash, "Mining the plasma proteome for disease applications across seven logs of protein abundance," *Journal of Proteome Research*, vol. 10, no. 1, pp. 46–50, 2011.

[5] P. G. Righetti, E. Boschetti, L. Lomas, and A. Citterio, "Protein equalizer technology : the quest for a "democratic proteome"," *Proteomics*, vol. 6, no. 14, pp. 3980–3992, 2006.

[6] V. Thulasiraman, S. Lin, L. Gheorghiu et al., "Reduction of the concentration difference of proteins in biological liquids using a library of combinatorial ligands," *Electrophoresis*, vol. 26, no. 18, pp. 3561–3571, 2005.

[7] P. G. Righetti, A. Castagna, P. Antonioli, and E. Boschetti, "Prefractionation techniques in proteome analysis: the mining tools of the third millennium," *Electrophoresis*, vol. 26, no. 2, pp. 297–319, 2005.

[8] P. G. Righetti, A. Castagna, F. Antonucci et al., "Proteome analysis in the clinical chemistry laboratory: myth or reality?" *Clinica Chimica Acta*, vol. 357, no. 2, pp. 123–139, 2005.

[9] P. G. Righetti, E. Boschetti, A. Zanella, E. Fasoli, and A. Citterio, "Plucking, pillaging and plundering proteomes with combinatorial peptide ligand libraries," *Journal of Chromatography A*, vol. 1217, no. 6, pp. 893–900, 2010.

[10] L. Sennels, M. Salek, L. Lomas, E. Boschetti, P. G. Righetti, and J. Rappsilber, "Proteomic analysis of human blood serum using peptide library beads," *Journal of Proteome Research*, vol. 6, no. 10, pp. 4055–4062, 2007.

[11] J. E. Bandow, "Comparison of protein enrichment strategies for proteome analysis of plasma," *Proteomics*, vol. 10, no. 7, pp. 1416–1425, 2010.

[12] C. Sihlbom, I. Kanmert, H. Von Bahr, and P. Davidsson, "Evaluation of the combination of bead technology with SELDI-TOF-MS and 2-D DIGE for detection of plasma proteins," *Journal of Proteome Research*, vol. 7, no. 9, pp. 4191–4198, 2008.

[13] E. Ernoult, A. Bourreau, E. Gamelin, and C. Guette, "A proteomic approach for plasma biomarker discovery with iTRAQ labelling and OFFGEL fractionation," *Journal of Biomedicine & Biotechnology*, vol. 2010, Article ID 927917, 8 pages, 2010.

[14] J. S. K. Au, W. C. S. Cho, T. T. Yip et al., "Deep proteome profiling of sera from never-smoked lung cancer patients," *Biomedicine and Pharmacotherapy*, vol. 61, no. 9, pp. 570–577, 2007.

[15] C. Marrocco, S. Rinalducci, A. Mohamadkhani, G. M. D'Amici, and L. Zolla, "Plasma gelsolin protein: a candidate biomarker for hepatitis B-associated liver cirrhosis identified by proteomic approach," *Blood Transfusion*, vol. 8, supplement 3, pp. s105–s112, 2010.

[16] M. Gatto, M. C. Bragazzi, R. Semeraro et al., "Cholangiocarcinoma: update and future perspectives," *Digestive and Liver Disease*, vol. 42, no. 4, pp. 253–260, 2010.

[17] T. Kondo and S. Hirohashi, "Application of highly sensitive fluorescent dyes (CyDye DIGE Fluor saturation dyes) to laser microdissection and two-dimensional difference gel electrophoresis (2D-DIGE) for cancer proteomics," *Nature Protocols*, vol. 1, no. 6, pp. 2940–2956, 2007.

[18] T. Okano, T. Kondo, T. Kakisaka et al., "Plasma proteomics of lung cancer by a linkage of multi-dimensional liquid chromatography and two-dimensional difference gel electrophoresis," *Proteomics*, vol. 6, no. 13, pp. 3938–3948, 2006.

[19] T. Kakisaka, T. Kondo, T. Okano et al., "Plasma proteomics of pancreatic cancer patients by multi-dimensional liquid chromatography and two-dimensional difference gel electrophoresis (2D-DIGE): Up-regulation of leucine-rich alpha-2-glycoprotein in pancreatic cancer," *Journal of Chromatography B*, vol. 852, no. 1-2, pp. 257–267, 2007.

[20] N. Zolotarjova, J. Martosella, G. Nicol, J. Bailey, B. E. Boyes, and W. C. Barrett, "Differences among techniques for high-abundant protein depletion," *Proteomics*, vol. 5, no. 13, pp. 3304–3313, 2005.

[21] R. C. Dwivedi, O. V. Krokhin, J. P. Cortens, and J. A. Wilkins, "Assessment of the reproducibility of random hexapeptide peptide library-based protein normalization," *Journal of Proteome Research*, vol. 9, no. 2, pp. 1144–1149, 2010.

[22] E. Mouton-Barbosa, F. Roux-Dalvai, D. Bouyssié et al., "In-depth exploration of cerebrospinal fluid by combining peptide ligand library treatment and label-free protein quantification," *Molecular and Cellular Proteomics*, vol. 9, no. 5, pp. 1006–1021, 2010.

[23] O. Beseme, M. Fertin, H. Drobecq, P. Amouyel, and F. Pinet, "Combinatorial peptide ligand library plasma treatment: advantages for accessing low-abundance proteins," *Electrophoresis*, vol. 31, no. 16, pp. 2697–2704, 2010.

[24] P. E. Scherer, S. Williams, M. Fogliano, G. Baldini, and H. F. Lodish, "A novel serum protein similar to C1q, produced exclusively in adipocytes," *Journal of Biological Chemistry*, vol. 270, no. 45, pp. 26746–26749, 1995.

[25] E. Hu, P. Liang, and B. M. Spiegelman, "AdipoQ is a novel adipose-specific gene dysregulated in obesity," *Journal of Biological Chemistry*, vol. 271, no. 18, pp. 10697–10703, 1996.

[26] K. Maeda, K. Okubo, I. Shimomura, T. Funahashi, Y. Matsuzawa, and K. Matsubara, "cDNA cloning and expression of a novel adipose specific collagen-like factor, apM1 (adipose most abundant gene transcript 1)," *Biochemical and Biophysical Research Communications*, vol. 221, no. 2, pp. 286–289, 1996.

[27] Y. Nakano, T. Tobe, N. H. Choi-Miura, T. Mazda, and M. Tomita, "Isolation and characterization of GBP28, a novel gelatin-binding protein purified from human plasma," *Journal of Biochemistry*, vol. 120, no. 4, pp. 803–812, 1996.

[28] Y. Matsuzawa, T. Funahashi, S. Kihara, and I. Shimomura, "Adiponectin and metabolic syndrome," *Arteriosclerosis, Thrombosis, and Vascular Biology*, vol. 24, no. 1, pp. 29–33, 2004.

[29] J. Spranger, A. Kroke, M. Möhlig et al., "Adiponectin and protection against type 2 diabetes mellitus," *The Lancet*, vol. 361, no. 9353, pp. 226–228, 2003.

[30] D. M. Maahs, L. G. Ogden, G. L. Kinney et al., "Low plasma adiponectin levels predict progression of coronary artery calcification," *Circulation*, vol. 111, no. 6, pp. 747–753, 2005.

[31] E. E. Calle, C. Rodriguez, K. Walker-Thurmond, and M. J. Thun, "Overweight, obesity, and mortality from cancer in a prospectively studied cohort of U.S. Adults," *New England Journal of Medicine*, vol. 348, no. 17, pp. 1625–1638, 2003.

[32] T. Arano, H. Nakagawa, R. Tateishi et al., "Serum level of adiponectin and the risk of liver cancer development in chronic hepatitis C patients," *International Journal of Cancer*, vol. 129, no. 9, pp. 2226–2235, 2011.

[33] C. Duggan, M. L. Irwin, L. Xiao et al., "Associations of insulin resistance and adiponectin with mortality in women with breast cancer," *Journal of Clinical Oncology*, vol. 29, no. 1, pp. 32–39, 2011.

[34] T. Krechler, M. Zeman, M. Vecka et al., "Leptin and adiponectin in pancreatic cancer: connection with diabetes mellitus," *Neoplasma*, vol. 58, pp. 58–64, 2011.

[35] P. T. Soliman, X. Cui, Q. Zhang, S. E. Hankinson, and K. H. Lu, "Circulating adiponectin levels and risk of endometrial cancer: the prospective nurses' health study," *American Journal of Obstetrics and Gynecology*, vol. 204, no. 2, pp. 167.e1–167.e5, 2011.

[36] T. Yamaji, M. Iwasaki, S. Sasazuki, and S. Tsugane, "Interaction between adiponectin and leptin influences the risk of colorectal adenoma," *Cancer Research*, vol. 70, no. 13, pp. 5430–5437, 2010.

[37] P. Ferroni, R. Palmirotta, A. Spila et al., "Prognostic significance of adiponectin levels in non-metastatic colorectal cancer," *Anticancer Research*, vol. 27, no. 1 B, pp. 483–489, 2007.

[38] G. Li, L. Cong, J. Gasser, J. Zhao, K. Chen, and F. Li, "Mechanisms underlying the anti-proliferative actions of adiponectin in human breast cancer cells, MCF7-dependency on the cAMP/protein Kinase-A pathway," *Nutrition and Cancer*, vol. 63, no. 1, pp. 80–88, 2011.

[39] R. A. Skidgel, G. B. McGwire, and X. Y. Lix, "Membrane anchoring and release of carboxypeptidase M: implications for extracellular hydrolysis of peptide hormones," *Immunopharmacology*, vol. 32, no. 1-3, pp. 48–52, 1996.

[40] D. A. Davis, K. E. Singer, M. De La Luz Sierra et al., "Identification of carboxypeptidase N as an enzyme responsible for C-terminal cleavage of stromal cell-derived factor-1α in the circulation," *Blood*, vol. 105, no. 12, pp. 4561–4568, 2005.

[41] G. Candiano, V. Dimuccio, M. Bruschi et al., "Combinatorial peptide ligand libraries for urine proteome analysis: investigation of different elution systems," *Electrophoresis*, vol. 30, no. 14, pp. 2405–2411, 2009.

Antibody-based proteomics for esophageal cancer: Identification of proteins in the nuclear factor-κB pathway and mitotic checkpoint

Norihisa Uemura,[1,3,4] Yukihiro Nakanishi,[2] Hoichi Kato,[3] Masato Nagino,[4] Setsuo Hirohashi[1] and Tadashi Kondo[1,5]

[1]Proteome Bioinformatics Project, National Cancer Center Research Institute; [2]Pathology Division, National Cancer Center Research Institute, Tokyo 104-0045; [3]Division of Esophageal Surgery, National Cancer Center Hospital, Tokyo 104-0045; [4]Division of Surgical Oncology, Department of Surgery, Nagoya University Graduate School of Medicine, Nagoya 466-8550, Japan

(Received March 3, 2009/Revised May 12, 2009/Accepted May 18, 2009)

To identify the molecular background of esophageal cancer, we conducted a proteomics study using an antibody microarray consisting of 725 antibodies and surgical specimens from three cases. The microarray analysis identified 24 proteins with aberrant expression in esophageal cancer compared with the corresponding normal mucosa. The overexpression of 14 of the 24 proteins was validated by western blotting analysis of the same samples. These 14 proteins were examined by immunohistochemistry, in which nine proteins showed consistent results with those obtained by western blotting. Among the nine proteins, seven were localized in tumor cells, and two in infiltrating cells. The former included proteins associated with mitotic checkpoint control and the nuclear factor (NF)-κB pathway. Although mitotic checkpoint gene products (budding uninhibited by benzidazoles 1 homolog beta (BubR1) and mitotic arrest deficient-like 1 (Mad2)) have previously been reported to be involved in esophageal cancer, the association of NF-κB-activating kinase, caspase 10, and activator protein-1 with esophageal cancer has not been previously reported. These proteins play a key role in the NF-κB pathway, and NF-κB is a signal transduction factor that has emerged as an important modulator of altered gene programs and malignant phenotype in the development of cancer. The association of these proteins with esophageal cancer may indicate that mitotic checkpoint gene products and NF-κB play an important part in the carcinogenesis of esophageal cancer. (*Cancer Sci* 2009)

Esophageal cancer is the eighth most common cancer[1] and the sixth leading cause of cancer death worldwide.[2] Despite the use of modern surgical techniques in combination with radiotherapy and chemotherapy, early recurrence is common and the overall 5-year survival rate remains below 40%.[3–5] ESCC develops through a multistep process from dysplasia through carcinoma *in situ* to invasive carcinoma, and the acquisition of molecular alterations tightly corresponds to the dysplasia–carcinoma sequence.[6] However, the mechanisms of esophageal cancer progression remain largely obscure. The characterization of molecular alterations inherently linked to ESCC development and an in-depth understanding of the molecular mechanisms underlying carcinogenesis and growth control may therefore provide information relevant to early tumor detection, refined prognosis, and development of novel targeted therapeutics.

As the proteome is a functional translation of the genome, directly regulating cancer phenotypes, its study may further our understanding of esophageal cancer. Esophageal cancer research has made significant progress due to proteomics studies on two fronts to date. First, tissue proteomics have identified numerous intracellular proteins that had not been previously reported to be implicated in esophageal cancer. For instance, the use of two-dimensional polyacrylamide gel electrophoresis followed by mass spectrometry and database search led to the identification of the aberrant expression of proteins correlating with certain clinicopathological parameters in esophageal cancer.[7] Second, the use of proteomics tools has led to the discovery of a novel candidate plasma biomarker for early diagnosis.[8] This is important as the majority of esophageal cancer cases has advanced locally or has developed distant metastases by the time of diagnosis, rendering the cancer surgically inoperable,[9,10] and the existing plasma tumor markers (e.g. squamous cell carcinoma-related antigen (SCC), cinoembryonic antigen (CEA), and cytokeratin-19 fragments (CYFRA21-1)) have obvious limitations in terms of sensitivity and specificity in detecting patients with localized and resectable esophageal cancer.[11]

The major proteomics tools such as two-dimensional gel electrophoresis and mass spectrometry essentially have two major drawbacks. First, these techniques tend to uncover the proteins in the order of their expression level; the proteins with higher expression levels are more frequently observed than proteins with low abundance such as transcription factors, receptors, and growth factors. Second, the present approaches do not allow the systematic profiling of protein expression. The proteins are currently identified when their physical characteristics, such as the molecular weight and charge, fit the conditions of the proteomic methods, and such protein characteristics do not necessarily correlate with protein functions. As a consequence, pathway comprehensive approaches such as those identifying all proteins in certain molecular pathways cannot be carried out using the present proteomics tools. To partially address these drawbacks, multidimensional separation by liquid chromatography and gel electrophoresis were used to reduce sample complexity and increase the number of observable proteins. However, further improvements are still required to overcome the limitations of cancer proteomics.

The recently developed antibody-based proteomics may address the aforementioned limitations of cancer proteomics. A large-scale library of antibodies with high specificity and sensitivity may be used to detect the proteins with low expression levels, and thus enable pathway comprehensive analysis. For instance, a large-scale immunoblotting analysis with 900 well-characterized antibodies resulted in the identification of 102 deregulated proteins in pancreatic cancer cells.[12] An antibody proteomics project was launched to detect all proteins encoded by the human genome.[13] In addition to the characterization of antibodies already developed, the development of techniques for hundreds or thousands of antibodies will be the challenge in antibody-based proteomics.

In this paper, we examined the proteins with aberrant expression levels in esophageal cancer tissues and normal tissues using an antibody microarray. The antibody microarray is commercially

[5]To whom correspondence should be addressed. E-mail: takondo@ncc.go.jp

doi: 10.1111/j.1349-7006.2009.01230.x

available and enables comprehensive high-throughput studies. We validated the antibody microarray study results by western blotting and immunohistochemistry. Through the comparison between the normal mucosa and tumor tissues, we discussed the reproducibility of the antibody microarray results, the degree of inconsistency between the different methods, and the functional contribution of the identified members of the NF-κB pathway to esophageal cancer progression.

Materials and Methods

Patients. Tumor tissues (1T, 2T and 3T) and their adjacent normal mucosal tissues (1N, 2N and 3N) were collected from three cases of ESCC, which were surgically resected in 2007 and 2008 at the National Cancer Center Hospital. The resected tissues were snap frozen in liquid nitrogen and stored at –80°C until use. All cases were newly diagnosed as squamous cell carcinoma of the esophagus (ESCC). The patients did not receive anticancer treatment prior to surgery. All patients were male and in the seventh decade of their lives, and all tumors were located in the lower thoracic segment of the esophagus and were classified as T3N1 according to the International Union against Cancer TNM classification.[14] Only one case with distant lymph node metastasis was classified as M1.[14] This study was approved by the ethics committee of the National Cancer Center and written informed consent was obtained from the patients.

Antibody microarrays. The Panorama Antibody Microarray XPRESS Profilter725, XP725 was purchased from Sigma-Aldrich (St Louis, MO, USA). Seven hundred and twenty-five antibodies were spotted on each glass slide in 32 subarrays, each containing duplicate spots for 23 antibodies, as well as duplicate positive control spots for Cy3 and Cy5 (monoclonal antibodies labeled with Cy3 and Cy5), and duplicate negative controls, resulting in 1536 spots per slide. These antibodies represent families of proteins known to be involved in a variety of different biological pathways. Detailed information on each antibody can be obtained in the antibody specific datasheet found on the Sigma-Aldrich website at http://www.sigma.com/arrays.

Protein extraction. Frozen samples were crushed to powder with a CryoPress (Microtech Nichion, Shizuoka, Japan) under cooling with liquid nitrogen. The frozen powder was then treated with urea lysis buffer (7 mol/L urea, 2 mol/L thiourea, 3% CHAPS, and 1% Triton X-100). After centrifugation at 17 400 *g* for 10 min, the supernatant was used as the source of cellular proteins for protein expression studies. The protein concentrations ranged between 3.46 and 8.45 mg/mL.

Protein labeling and microarray assays. Briefly, 100 μg (77 μL) of protein extracted from each tumor and normal sample were labeled with Cy5 (Cy5 Mono Reactive Dye; GE Healthcare Biosciences, Uppsala, Sweden), using a scaled-down version of the protocol provided by the manufacturer. The protein extracts were mixed with 20 μL of 0.5 M sodium bicarbonate, pH 8.5. The labeling reaction was carried out for 30 min at room temperature. Labeled samples were purified from free excess dye using the Sigma Spin columns supplied with the antibody microarray kit. The 100 mg labeled protein samples (1 mg/ml) were applied onto the column, and centrifuged first for 2 min and then for 4 min at 800 *g*. The protein concentration of the recovered samples was adjusted to 1 mg/mL in 100 μL. Before hybridization, the dye-to-protein molar ratio was adjusted to 2.93–4.84 mol of dye/mol of protein according to the manufacturer's instructions. Labeled protein extracts were incubated on Panorama Ab Microarray slides (Sigma-Aldrich) for 30 min with moderate shaking. The slides were washed three times in PBS, in Tween 20 for 5 min, and immersed in water for 2 min. Finally, the slides were air dried and scanned with a laser scanner at the appropriate wave length (Typhoon Trio; GE Healthcare Biosciences).

Data analysis and identification of alterations. Microarray images were analyzed with the Array Vision software version 8.0 (GE Healthcare Biosciences). Fluorescence intensity measurements from each array element were compared with local background, and background subtraction was carried out. The reported value represents the average of all the pixels remaining in the spot, after first removing the pixels with density values that exceeded a threshold value set at four times the absolute deviation value above the median. This measure removes the influence of image artifacts, such as dust particles, on density estimation. The proteins showing ≥2.5-fold difference in expression in more than two cases of three were deemed significant.

Western blotting. Five μg of each protein sample was separated by SDS-PAGE on a 10–12.5% polyacrylamide gradient gel and subsequently blotted on a nitrocellulose membrane. Immunoblot analysis was carried out using the antibodies listed in Table 1 and horseradish peroxidase-conjugated secondary antibodies (1:1000; GE Healthcare Biosciences). Antibody–antigen complexes were visualized with an ECL system (GE Healthcare Biosciences) using LAS 3000 (Fuji Film, Tokyo, Japan). The intensity of the protein bands was quantified and the relative intensity of the examined proteins was calculated on the basis of the intensity of the actin bands on the same membrane.

Immunohistochemistry and tissue microarray. The cellular localization of the proteins was examined immunohistochemically on methanol-fixed, paraffin-embedded tissues using the Dako REAL EnVision Detection System (DAKO, Glostrup, Denmark) following the manufacturer's instructions. In brief, the sections were deparaffinized, dehydrated, and blocked with 0.3% H_2O_2 in methanol for 30 min to remove endogenous peroxidase activity. The sections were autoclaved in 10 mM citrate buffer (pH 6.0) at 121°C for 10 min. The primary antibodies and dilutions used are shown in Table 1.

We obtained two commercial tissue microarrays (ES801; US Biomax, Rockville, MD, USA; and A218(II) AccuMax array; ISU ABXIS, Seoul, Korea) including 40 and 30 esophageal cancer cases with matched normal adjacent tissue, respectively, and used them to examine the expression of the identified proteins and their relationship with the corresponding clinicopathological data. The sex, age, and histological grade were available for all 70 cases on the tissue microarrays, whereas the tumor stage, lymph node metastasis status, distant metastasis status, and tumor size were only available for the 30 cases on the A218(II) array.

mRNA expression analysis. Total RNA was isolated from six ESCC tissues using an Isogen kit (Nippon Gene, Toyama, Japan). The integrity of the RNA was determined on the Agilent 2100 Bioanalyser using the RNA 6000 Nano Kit (Agilent Technologies, Palo Alto, CA, USA). RNA expression analysis was carried out using the GeneChip 3' IVT expression kit (Affymetrix, Santa Clara, CA, USA) according to the supplier's protocol. Labeled targets were hybridized to the GeneChip Human Genome U133 Plus 2.0 Array. Gene expression analysis was carried out using the Affymetrix GeneChip Command Console Software. Experimental data were quantile normalized in Expression Console using the RMA algorithm for probe set summarization. The maximal signal was adopted for subsequent analysis when there were multiple probes corresponding to the same protein.

Statistical analysis. The numerical data were imported into the Expressionist software (Genedata, Basel, Switzerland) for scatter plotting and calculation of the correlation coefficient. The correlation between protein expression and clinicopathological features was evaluated using the Fisher exact test for categorical variables and the Mann–Whitney *U*-test for continuous variables. *P*-value differences of <0.05 were considered to be significant. Statistical analyses were carried out using the SPSS 11.0 statistical package (SPSS, Chicago, IL, USA).

doi: 10.1111/j.1349-7006.2009.01230.x

Table 1. List of the proteins found to be overexpressed in the microarray analysis and examined by western blotting and immunohistochemistry

No.	Antibody commercial name	Company	Product no.	Dilution	
				Western blotting	Immunohistochemistry
1	Acetylated protein	Sigma	A5463	1: 100	–
2	Actin	Sigma	A5060	1: 1000	–
3	AP-1	Sigma	A5968	1: 200	1: 5000
4	AP-2a	Sigma	A0844	1: 100	1: 500
5	BAD	BD Biosciences	610391	1: 500	1: 500
6	BUBR1	BD Biosciences	612502	1: 500	1: 500
7	Calbindin-D	Sigma	C7354	1: 250	–
8	Caspase 10	Sigma	C8351	1: 250	1: 500
9	Cdk1	Sigma	C4973	1: 250	1: 500
10	phosph-β-catenin	Sigma	C4231	1: 250	1: 5000
11	Cytokeratin 18	Sigma	C1399	1: 500	–
12	HABH3	Sigma	A8353	1: 250	1: 500
13	hnRNP-U	Sigma	R6278	1: 500	1: 500
14	Mad 2	Sigma	M8694	1: 250	1: 5000
15	NAK	Sigma	N2661	1: 250	1: 50
16	NG2	Sigma	N8912	1: 250	1: 50
17	b-NOS	Sigma	N2280	1: 500	1: 200
18	NGFb	Sigma	N3279	1: 100	–
19	RAB 9	ABR-Affinity Bioreagents	MA3-067	1: 250	1: 200
20	Protein phosphatase 2A alpha	Sigma	P8998	1: 250	–
21	Protein Tyrosine Phosphatase	Sigma	P9109	1: 250	–
22	phospho-Pyk2	Sigma	P7114	1: 250	–
23	SKK2	Abnova	H00005606-M02	1: 100	–
24	Tropomyosin (Sarcimatic)	Sigma	T9283	1: 100	–

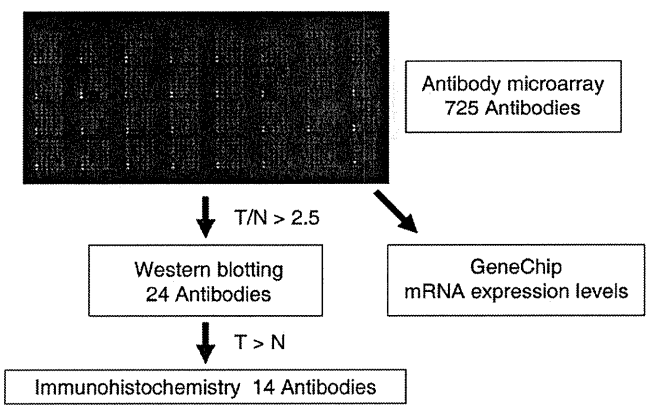

Fig. 1. Scheme showing the experimental flow: the antibody microarray analysis results were validated using western blotting and immunohistochemistry. N, normal; T, tumor.

Results

Antibody microarray performance. The protein contents of surgical specimens from three patients diagnosed with ESCC were extracted. The scanned image of an antibody microarray for a representative tumor extract (1T) is shown in Figure 1. The shape of the spots, the dynamic range of the intensity response, and the signal-to-noise ratio, as well as the positive and negative controls were routinely checked. The reproducibility of the results was monitored by comparing duplicate spots on the same slide. The scatter plot demonstrated that the intensity values of 63.1–94.1% of the antibody spots was scattered within a twofold difference, and that the correlation coefficient was 0.7172–0.9332 in all six samples examined (Fig. 2). Although spot intensity showed high reproducibility for spots with higher intensity in the microarray slide, it showed poor reproducibility for spots with lower intensity, even when adjacent duplicated spots on the same slide were compared.

Differential protein expression analysis. We initially searched for proteins with upregulated expression in esophageal cancer compared to the corresponding normal reference mucosa. Twenty-four proteins, including two non-unique proteins (whole acetylated proteins and protein tyrosine phosphatases), showed a notable upregulation (more than 2.5-fold change in at least two samples) in the tumor compared to the normal tissues (Table 2). No proteins showed notable downregulation in the tumor tissues compared with their normal reference mucosa. We classified the identified proteins based on their biological function according to Gene Ontology web site and literature searching by the author. Proteins associated with signal transduction were the most frequently identified, followed by those involved in apoptosis, cell cycle, and the cytoskeleton (Table 2). The locus of the identified proteins was variable, and absence of constant chromosomal localization was noted (Table 2).

Western blotting analysis. The 24 proteins identified in the microarray analysis were validated using western blotting. Fourteen of the 24 proteins showed overexpression in the tumor tissues, the results being consistent with the results of microarray analysis. Six proteins showed discordant results; five proteins showed inverse expression compared to the microarray results, whereas actin was found to be consistently expressed in the tumor and normal tissues in western blotting (Table 3; Fig. 3). Four proteins were undetectable in western blotting.

The scattergram (Fig. 4) demonstrates the correlation between the intensity of the duplicate antibody signals of the 24 proteins, in relation to the consistency between western blotting and antibody microarray experiments. The intensity values of the proteins found to be upregulated in tumor tissues in the microarrays showed high reproducibility, irrespective of whether these microarray results were discordant ($R = 0.7666$) or concordant ($R = 0.6921$) with western blotting results, or whether these proteins were not detected in western blotting ($R = 0.6317$). We concluded that reproducibility of the antibody microarray